Conformational change in cytochrome P450 reductase adsorbed at a Au(110)—phosphate buffer interface induced by interaction with nicotinamide adenine dinucleotide phosphate

C. I. Smith,[1] J. H. Convery,[1] P. Harrison,[1] B. Khara,[2] N. S. Scrutton,[2] and P. Weightman[1,*]

[1]*Department of Physics, Oliver Lodge Laboratory, University of Liverpool, Liverpool, L69 7ZE, United Kingdom*

[2]*Faculty of Life Sciences, University of Manchester, Manchester Institute of Biotechnology, 131 Princess Street, Manchester, M1 7DN, United Kingdom*

(Received 9 April 2014; published 13 August 2014)

Changes observed in the reflection anisotropy spectroscopy (RAS) profiles of monolayers of cytochrome P450 reductase adsorbed at Au(110)–electrolyte interfaces at 0.056 V following the addition of nicotinamide adenine dinucleotide phosphate ($NADP^+$) are explained in terms of a simple model as arising from changes in the orientation of an isoalloxazine ring located in the flavin mononucleotide binding domain of the protein. The model also accounts for the changes observed in the RAS as the potential applied to the Au(110) surface is varied and suggests that differences in the dependence of the RAS profile of the adsorbed protein on the potential applied to the electrode in the absence and presence of $NADP^+$ are explicable as arising from a competition between the applied potential acting to reduce the protein and the $NADP^+$ to oxidize it.

DOI: 10.1103/PhysRevE.90.022708 PACS number(s): 87.14.E−, 87.64.K−, 87.15.hp

I. INTRODUCTION

This work is part of a long-term program aimed at developing the potential of the optical technique of reflection anisotropy spectroscopy (RAS) as a real time monitor of conformational changes in proteins adsorbed on surfaces [1–4]. There has been considerable progress in determining the structure of proteins using techniques such as x-ray diffraction but, due to the dearth of experimental techniques, less progress in measuring the conformational changes that are the key to their function. There is a particular need for an experimental technique that can measure conformational changes occurring in "real time" making it possible to monitor changes occurring during a chemical change such as an electron transfer event. The results of research on small molecules adsorbed at Au(110)–phosphate buffer interfaces indicates that RAS has the potential to fill this gap in experimental capabilities [5–7]. The protein chosen for these studies is the human flavoprotein cytochrome P450 reductase (CPR) [8–11]. It is an electron transfer flavoprotein that in living systems is anchored to the membrane of the endoplasmic reticulum and which carries out its electron transfer function by large changes in the relative orientation of two structural domains of the protein: the flavin adenine dinucleotide (FAD) and flavin mononucleotide (FMN) binding domains. The aim of the research program is to directly monitor changes in the relative orientation of these domains as electrons are transferred or withdrawn from the protein by varying the potential applied to the Au(110) electrode and thus altering the electrochemical driving force for electron transfer across the CPR-Au(110) interface.

In earlier work we have established the conditions under which ordered monolayers of CPR are adsorbed at Au(110)–phosphate buffer interfaces [2–4]. The experiments employed an engineered form of CPR with a cysteine residue on the solvent accessible surface at the location of the Pro-499 residue (P499C) as described previously [2]. The cysteine residue facilitated the adsorption through the formation of a Au-S bond. It was found, using RAS, that monolayers adsorbed on Au(110) at applied potentials of −0.652 and 0.056 V, which are, respectively, the potentials at which P499C is fully reduced or oxidized in solution [2,4], were orientated with the optical transitions that give rise to the RAS profile lying in a plane that is orientated roughly normal to the surface and parallel to either the $[1\bar{1}0]$ or [001] axes of the Au(110) surface. It is clear that the long-range order of the Au(110) surfaces at the two applied potentials plays an important role in inducing the formation of ordered monolayers of adsorbed P499C [4].

This work reports the results of experiments in which nicotinamide adenine dinucleotide phosphate ($NADP^+$), the oxidized form of the electron transfer reducing coenzyme molecule NADPH that facilitates the functional activity of CPR, is added to the solution above ordered layers of P499C adsorbed at Au(110)–phosphate buffer interfaces. It is shown that $NADP^+$ induces changes in the RAS profiles of the adsorbed molecules that can be interpreted in terms of a simple model as arising from a change in the orientation of the FMN domain. This model also accounts for the changes observed in the RAS as the potential applied to the Au(110) surface is varied and suggests that differences in the dependence of the RAS profile of the adsorbed protein on the potential applied to the electrode in the absence and presence of $NADP^+$ is explicable as arising from a competition between the applied potential acting to reduce the protein and the $NADP^+$ to oxidize it.

II. EXPERIMENTAL SECTION

As in previous work [1–7] experiments were performed on a Au(110) single crystal of 99.999% purity in the form of a disk of diameter 10 mm and 2 mm thick with an exposed surface area of 0.5 cm^2. The orientation of the crystal by x-ray diffraction, its preparation by polishing and flame annealing, and insertion into the electrochemical cell have been described previously [1,2,5–7]. The electrochemical cell, potentiostat, referencing of potentials to a saturated calomel electrode

*Author to whom correspondence should be addressed: peterw@liverpool.ac.uk

(SCE), and the RAS instrument have also been described previously [1–7,12,13]. The RAS instrument yields a linear optical signal that is the difference in reflectivity from two orthogonal directions in the surface of plane polarized light at normal incidence and near normal reflection from the crystal. For a cubic substrate, this geometry results in a cancellation of the bulk signal by symmetry and RAS becomes a probe of surface anisotropy [12]. The measured RA signal from 1.5 to 5.5 eV is given by

$$\left(\frac{\Delta r}{r}\right) = 2\left(\frac{r_{[1\bar{1}0]} - r_{[001]}}{r_{[1\bar{1}0]} + r_{[001]}}\right), \qquad (1)$$

where $r_{[1\bar{1}0]}$ and $r_{[001]}$ are the reflection coefficients in the $[1\bar{1}0]$ and [001] directions in the (110) surface, respectively, and $\frac{r}{2}$ is the average of these quantities. In this work we are concerned only with the real part (Re) of the complex expression shown in (1) [12]. This is assumed in subsequent expressions but not explicitly stated.

As in the previous work [1–7], the solutions used were NaH_2PO_4 and K_2HPO_4 (BDH, Analar grade) prepared with Millipore ultrapure water (18 MΩ cm) and made oxygen free by purging with argon prior to use. The CPR was engineered to have a cysteine residue at the location of the Pro-499 residue found in the wild-type enzyme as described previously [1,2], and the potentials of the oxidized form, 0.056 V, and the four successively reduced forms, −0.376, −0.465, −0.557, and −0.652 V, of the P499C variant have been determined [2]. The concentration 4.2 m*M* of $NADP^+$ added to the CPR-Au(110) assembly was sufficient to saturate all surface molecules of CPR based on the known saturation constant ($Ks \sim 1.6$ m*M*) for the CPR-$NADP^+$ complex [10]. The RAS profiles of the $NADP^+$-P499C-Au(110) assembly were recorded in the sequence of applied potentials 0.056, 0.376, −0.465, −0.557, and −0.652 V.

Finally in a control experiment $NADP^+$ was added to the electrochemical cell and adsorbed onto a freshly prepared Au(110)–phosphate buffer interface at 0.056 V. The RAS profiles were recorded as the potential applied to the Au(110) electrode was varied in the same sequence as in the experiments described above.

III. RESULTS

The RAS profile of the initial Au(110)–electrolyte interface was obtained at an applied potential of 0.056 V, corresponding to the oxidized form of P499C in solution, and is shown in Fig. 1. A solution of P499C was then added to the electrochemical cell at a concentration and *p*H that are known to lead to the formation of an ordered monolayer on the Au(110) surface; the RAS profile of this surface was obtained before and after the addition of $NADP^+$ to the cell.

The RAS profile of the Au(110) surface obtained at an applied potential of 0.056 V is almost identical to those reported earlier [2–4] except for the position of the zero on the vertical scale. The latter is sensitive to minutes of arc in the alignment of the first polarizer of the RAS instrument and its variation in these experiments has no influence on the interpretation of the results, which is concerned with differences between spectra taken at the same setting of the polarizer. As noted previously the RAS profile of the Au(110) surface obtained at an applied potential of 0.056 V is very similar to that observed from a (1Í1) anion induced Au(110) surface structure [14].

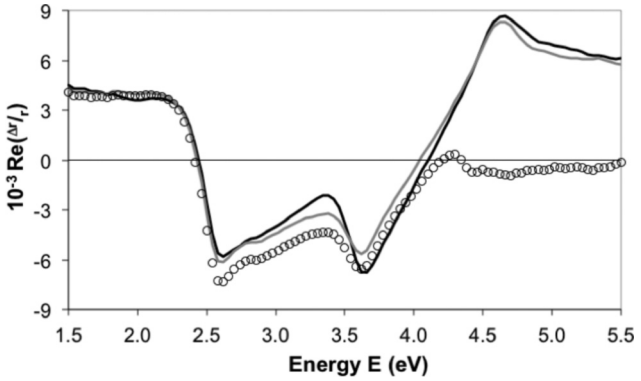

FIG. 1. RA spectra of Au(110) (black line), Au(110) + P499C CPR (gray line), and Au(110) + P499C CPR + $NADP^+$ (○) all recorded at 0.056 V in 0.1 M NaH_2PO_4-K_2HPO_4 at *p*H 7.2.

The RAS profiles obtained following the addition of P499C and $NADP^+$ to the cell are also shown in Fig. 1. The RAS profile of the adsorbed P499C on the Au(110) surface is almost identical to those reported earlier [2,3]. $NADP^+$ absorbs strongly in solution above ∼4.2 eV and this is the origin of the falloff in intensity of the RAS signal above 4.2 eV when $NADP^+$ is added to the cell. In order to bring out the spectral changes in the RAS signals more clearly the spectra above 4.2 eV are omitted from Fig. 2. This figure shows the difference between the RAS profiles of the P499C-Au(110) and the Au(110) surfaces together with the difference between the RAS profiles of $NADP^+$-P499C-Au(110) and the Au(110) surface. The difference between these two differences, which brings out the effect of the $NADP^+$ on the RAS of the P499C-Au(110) surface, is also shown in Fig. 2.

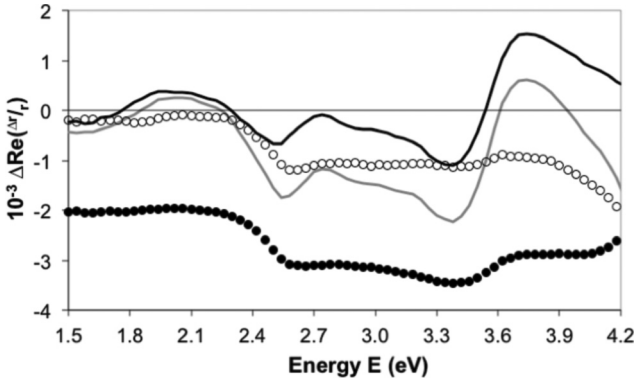

FIG. 2. RA spectra of P499C CPR (black line) and P499C CPR + $NADP^+$ (gray line) obtained after subtracting the RAS of Au(110) using the results shown in Fig. 1. The contribution of $NADP^+$ (○) is deduced as the difference between the RAS shown by the gray and black lines. Also shown is the control experiment of the RA spectrum of 5 m*M* $NADP^+$ adsorbed on Au(110) after subtracting the RAS of Au(110) (●). This profile has been shifted down by two units on the vertical axis and shown on a reduced scale, one fifth of that of the other profiles. All recorded at 0.056 V in 0.1*M* NaH_2PO_4-K_2HPO_4 at *p*H 7.2.

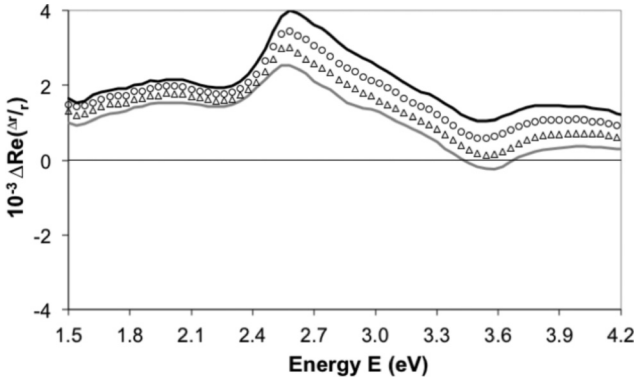

FIG. 3. The RAS profiles obtained for Au(110) + P499C CPR at −0.376 V (gray line), at −0.465 V (△), −0.557 V (○), and −0.652 V (black line) obtained after subtracting the RAS of Au + P499C CPR at 0.056 V vs SCE in 0.1 M NaH_2PO_4-K_2HPO_4 at *p*H 7.2. This figure is generated from the results shown in Fig. 3(a) of Ref. [3].

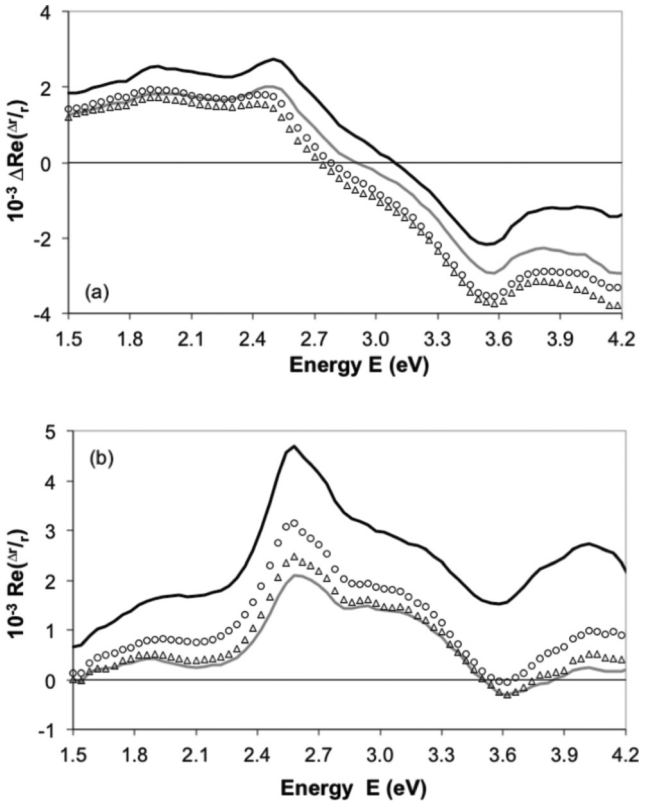

FIG. 4. (a) The RAS profiles obtained for Au(110) + P499C CPR + $NADP^+$ at −0.376 V (gray line), at −0.465 V (△), −0.557 V (○), and −0.652 V (black line) obtained after subtracting the RAS of Au + P499C CPR + $NADP^+$ at 0.056 V vs SCE in 0.1 *M* NaH_2PO_4-K_2HPO_4 at *p*H 7.2. These figures are generated from the results obtained in this work. (b) The RAS profiles obtained for Au(110) + $NADP^+$ at −0.376 V (gray line), at −0.465 V (△), −0.557 V (○), and −0.652 V (black line), obtained after subtracting the RAS of Au + $NADP^+$ at 0.056 V vs SCE in 0.1*M* NaH_2PO_4-K_2HPO_4 at *p*H 7.2

It was found earlier that the RAS profiles of adsorbed P499C depend on the applied potential and in particular on the sequence in which the potentials, −0.376, −0.465, −0.557, and −0.652 V corresponding to the $1e^-$, $2e^-$, $3e^-$, and $4e^-$ reduced forms of P499C in solution [3] were applied to the Au(110) electrode [3]. In order to explore the effect of changes in the applied potential on the RAS profile of the adsorbed molecules in the presence of $NADP^+$, subsequent RAS profiles, following adsorption at 0.056 V, were recorded in the sequence −0.376, −0.465, −0.557, and −0.652 V corresponding to the $1e^-$, $2e^-$, $3e^-$, and $4e^-$ reduced forms of P499C in solution [3]. In the experiments on P499C reported in [3] and on P499C interacting with $NADP^+$ reported here the applied potential was stepped and after each step the RAS recorded. Each experiment took ∼7 min, which is too slow to monitor dynamic changes.

A useful way to capture the dependence of the RAS profiles on the applied potential is to subtract the RAS profile obtained following the initial adsorption of the protein from the RAS profiles obtained as the potential is varied through the redox potentials of the protein. These results are shown in Fig. 3 for the profiles reported in Fig. 3(a) of Ref. [3] in which the P499C was adsorbed on the Au(110) at 0.056 V. The results obtained from these studies, in which P499C was also adsorbed at 0.056 V and then $NADP^+$ was added to the cell before the applied potentials were varied, are shown in Fig. 4. In each of Figs. 3 and 4 the applied potentials were varied in the same sequence, 0.056, −0.337, −0.465, −0.557, and −0.652 V, which correspond to the reduction of the protein in solution by one, two, three, and four electrons, respectively.

In the control experiments the RAS of $NADP^+$ on Au(110) at 0.056 V was found to be similar to the RAS of adenine adsorbed on the same surface at 0.0 V (Fig. 2 of Ref. [6]) which is not surprising given the similarity of the structure of the two molecules. Since the P449C may not completely cover the Au(110) surface we cannot rule out the possibility that some $NADP^+$ interacting with bare Au(110) surface contributes to the RAS profile of $NADP^+$-P499C-Au(110). However such a contribution is unable to account for the spectral changes that are observed above ∼2.6 eV when $NADP^+$ is added to P499C-Au(110) (Fig. 2). Furthermore the RAS profiles of $NADP^+$ on Au(110) show a quite different dependence on the potential applied to the Au(110) electrode compared to that of $NADP^+$-P499C-Au(110). In particular the differences between these RAS profiles do not become significantly negative at any point in the spectral range and show quite different line shapes to those observed for $NADP^+$-P499C-Au(110) (Fig. 4). We conclude that we can discount any significant influence on the results arising from the direct interaction of $NADP^+$ with Au(110).

IV. DISCUSSION

The changes in the RAS profiles of Au(110)–electrolyte interfaces induced by the adsorption of P499C have been discussed in detail and attributed to the introduction of a peak at 2.54 eV, that arises from the Au-S bond linking the molecules to the Au surface, optical transitions associated with the P499C molecule that have been identified from studies of the optical spectra of the isoalloxazine rings [15–18], the UV-visible absorption spectrum of the P499C molecule in solution, and the changes in this absorption spectrum as the redox potential

is varied [3]. The isoalloxazine rings are located in the FAD and FMN domains of the protein [2–4]. They give rise to two broad spectral features that can be identified in the RAS profile, one, denoted I, between 2.4 and 3.0 eV that peaks at 2.7 eV and a second, denoted II, between 3.0 and 3.8 eV, the energy of which is dependent on the redox potential. The isoalloxazine rings also give rise to a strong peak centered on 4.5 eV in the absorption spectrum of P499C in solution [15–18] that may be the origin of a feature observed to high energy in the RAS profile of the adsorbed P499C [3]. However, it is not possible to be certain of this identification because the absorption spectrum of P499C in solution includes a very strong contribution in this region of the spectrum arising from the large number of aromatic residues in the molecule [2]. The contribution from aromatic residues is considerably weakened in the RAS profile due to the lack of order in the orientation of these molecules in the structure of the protein, but it is possible that some residual order in the adsorbed monolayer leads to a contribution in the high-energy region of the RAS profile of the adsorbed species. The absorption spectrum of P499C in solution also shows a contribution between 1.8 and 2.3 eV, denoted L, the intensity of which is very dependent on the redox state of the molecule. The origin of this contribution is unknown but it can be clearly identified in the RAS profile of the adsorbed molecule.

In analyzing the effects of the addition of $NADP^+$ on the RAS profiles of the adsorbed molecules it is important to note that while changes in the redox state of the CPR protein in solution gives rise to changes in the intensity of transitions in the absorption spectrum [3], experiments on the isoalloxazine rings in solution show that the directions of the dipole transitions with respect to the molecular axes are essentially independent of the oxidation state of the isoalloxazine ring [15]. This means that any $NADP^+$ induced change in the RAS profiles associated with the isoalloxazine rings will arise from changes in the orientations of the isoalloxazine rings as a whole with respect to the Au(110) surface.

The changes in the RAS of the monolayer of P499C adsorbed at the Au(110)–electrolyte interface due to the addition of $NADP^+$ are shown in Figs. 1 and 2. They are associated with features in the RAS of the adsorbed monolayer that are dependent on the potential applied to the Au(110) and, by implication, with the redox state of the protein [3]. There is a very small change in the intensity of the low-energy feature, L, following the addition of $NADP^+$ and a stronger change, roughly evenly distributed, across the whole range of the profile to higher energy that is associated with the contributions I and II of the isoalloxazine rings to the spectrum of the monolayer of P499C.

$NADP^+$ acts to remove electrons from CPR in solution by binding to the FAD-$NADP^+$ domain. The effects on the absorption spectrum of the CPR molecule in solution as CPR is reduced with the general reductant sodium dithionite are shown in Fig. 4 of Ref. [3]. These changes in the absorption spectrum are similar to those observed during reduction of CPR with NADPH [11]. A previous analysis concluded that in monolayers of P499C adsorbed at Au(110)–electrolyte interfaces at 0.056 V the molecules were not completely oxidized even though this potential is found to oxidize the molecule in solution [3]. It may be that the applied potential required to oxidize the molecule on the Au(110) surface is more extreme than that required in solution. Alternatively this difference could arise from incomplete electrical contact between the Au(110) surface and the FMN and FAD domains of the adsorbed molecules. In the fully oxidized molecules in solution the FMN and FAD domains of P499C adopt a "closed" structure that is mediated by interaction with $NADP^+$ [10]. Since the P499C molecules adsorbed on Au(110) are not fully oxidized at 0.056 V it is reasonable to suppose that the FMN and FAD domains of the adsorbed molecules are not completely closed and that the action of $NADP^+$ on the adsorbed monolayer is to complete the oxidation and close the domains. This will result in a change in the orientation of the isoalloxazine rings and is a likely explanation of the changes in the RAS profile of the adsorbed proteins induced by the addition of $NADP^+$ to the electrochemical cell (Figs. 1 and 2).

A. A model for the $NADP^+$ induced changes in the RA spectrum of P499C-Au(110)

We now propose a simple model [19] that explains the changes in the RAS profile of P499C adsorbed at the Au(110)–phosphate buffer interface by the interaction with $NADP^+$. The model exploits the sensitivity of RAS to the directions of dipole transitions with respect to a surface [5–7,10–24]. Previous work leads us to expect that each molecule of P499C is orientated on the surface with the planes of the two isoalloxazine rings vertical to the surface and orientated along one of the principal axes of the Au(110) surface. The FAD domain is secured to the surface through a Au-S bond and we assume that this fixes the orientation of the isoalloxazine ring in this domain. We assume the FMN domain is free to rotate and that during this rotation the two isoalloxazine rings maintain the same vertical plane. In the fully oxidized form the molecule is closed and we assume that in this form the long axes of both isoalloxazine rings are vertical to the surface. The orientation of the isoalloxazine rings in the fully oxidized state in this model is indicated in Fig. 5(a) where the supporting structure of the domains is indicated schematically. The directions of the dipole transitions I and II are indicated in the figure. Since these directions are fixed relative to each other we specify only one angle, α_1, for their orientation with respect to a principal axis of the Au(110) surface. All the theoretical calculations agree that the dipole moments of both transitions, I and II, are orientated close to the long axes of the isoalloxazine rings with three different theoretical results giving angles relative to the long axis of 0°, 15°, and 32° [15–17] for I, and 11°, 10°, and 10° [15–17] for II. In the fully oxidized state these angles correspond to values of α_1 of 90°, 75°, and 58°, respectively, for I, and of 79°, 80°, and 80°, respectively, for II with respect to one of the principal axes of the Au(110) surface. The contribution of transitions I and II to the RAS profile will vary as $\cos\alpha_1$. We explain the differences between the RAS of P499C-Au(110) and $NADP^+$-P499C-Au(110) in the spectral region above 2.4 eV (Figs. 1 and 2) as arising from a change in α_1 induced by the interaction of $NADP^+$ with the P499C adsorbed on the Au(110) surface.

We now assume that without loss of generality α_1 is measured with respect to the [001] direction in the Au(110)

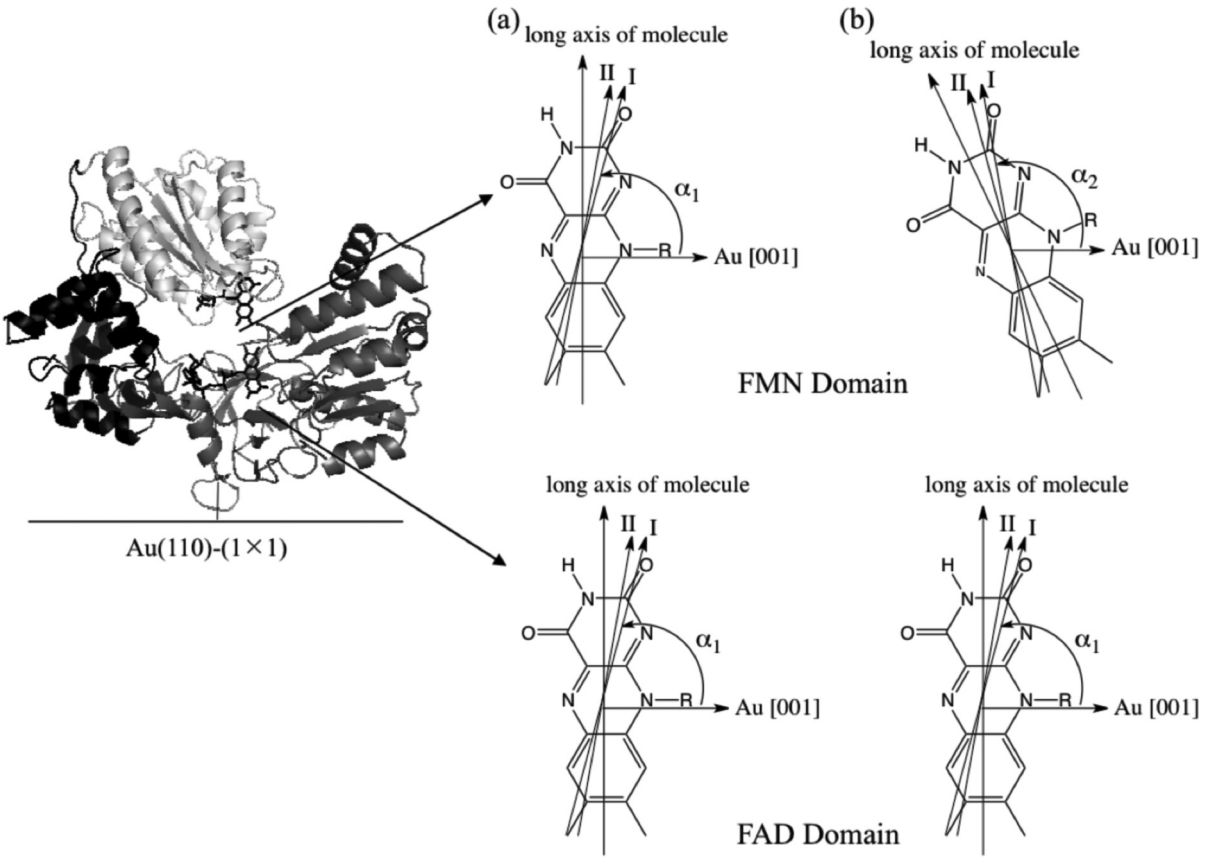

FIG. 5. A molecular graphics ribbon diagram representation of the structure of cytochrome P450 reductase in the closed form is shown on the left. The suggested orientations of the isoalloxazine rings in the FMN and FAD domains in the closed oxidized form and the more open reduced form are shown in (a) and (b), respectively, with respect to the Au[001] direction. The directions of the transition dipoles for the I and II contributions to the optical spectrum of the isoalloxazine rings are taken from Ref. [16].

surface. The contributions to Δr in Eq. (1) arise from the Au(110) surface, the low-energy transition L, and the isoalloxazine rings which we denote as IR.

$$\Delta r = \Delta r\,(\mathrm{Au}) + \Delta r\,(L) + \Delta r\,(\mathrm{IR})\,. \tag{2}$$

Applying Eq. (2) to the difference between the RAS obtained for the $NADP^+$-P499C-Au(110) and P499C-Au(110) specimens shown by the circles in Fig. 2 we expect the contribution from the Au(110) surface to cancel. It is possible that the low-energy feature, L, is a weak previously unidentified $n\rightarrow\pi$ contribution from the isoalloxazine rings (IR) which is not observed in solution but is enhanced by the ordering of the molecules on the Au(110) surface. In this case the transitions will be in a plane at right angles to that of the isoalloxazine rings. In any case this contribution to the difference in the RAS of these two systems, represented by the circles in Fig. 2, is very small (Fig. 2) and can be ignored. We are left with the difference between the RAS signals of these two systems as arising from the contributions from the isoalloxazine rings.

$$\begin{aligned}&\Delta r_{(\mathrm{P499C+NADP^+})} - \Delta r_{(\mathrm{P499C})}\\ &\quad = \Delta r_{(\mathrm{P499C+NADP^+})}(\mathrm{IR}) - \Delta r_{(\mathrm{P499C})}(\mathrm{IR}).\end{aligned} \tag{3}$$

Assuming the FAD domain is fixed then the contribution from its associated isoalloxazine ring will cancel in Eq. (3) leaving only the contribution from the isoalloxazine ring in the FMN domain. Since the protein is not fully oxidized before the addition of $NADP^+$ the molecule will not be completely closed on the surface initially and we assume that the orientations of the optical dipole transitions depicted in Fig. 5(b) state can be specified by an angle α_2 with respect to the [001] direction. Assuming the addition of $NADP^+$ completes the oxidation of P499C on the surface then this will close the molecule and the transitions depicted in Fig. 5 will change their orientation from α_2 to the smaller angle α_1. From Eq. (1), Eq. (3) now becomes

$$\Delta r_{(\mathrm{P499C+NADP^+})} - \Delta r_{\mathrm{P499C}} = D\,(\cos\alpha_2 - \cos\alpha_1) \tag{4}$$

where D is a constant which will be different for I and II. Whatever the values of α_1 describing the orientations of I and II the corresponding angles of α_2 will all be larger, since they are increased by the angle by which the isoalloxazine ring deviates from the vertical (Fig. 5). Consequently the right-hand side of Eq. (4) should be negative across the whole spectral range above ~2.4 eV as observed (Fig. 2).

B. Application of the model to the dependence of the RA spectrum of P499C-Au(110) on the applied potential

The success of this simple model in explaining the changes induced in the RAS of the P499C-Au(110) system by the addition of $NADP^+$ raises the possibility that it can be used

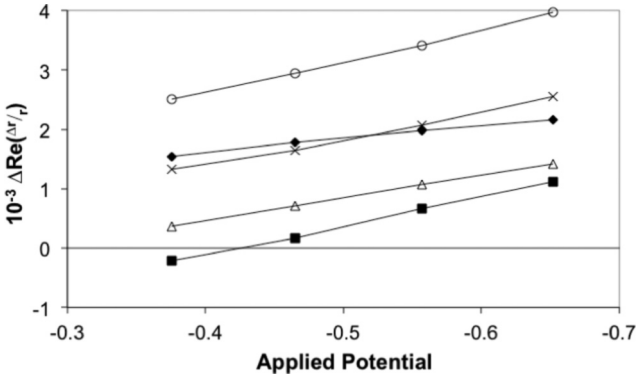

FIG. 6. Changes in peak intensity from Fig. 3 at 2.0 eV (♦), 2.6 eV (○), 3.0 eV (X), 3.6 eV (■), and 4.0 eV (△) as the P499C CPR is reduced on the surface of the Au(110) electrode in 0.1*M* NaH_2PO_4-K_2HPO_4 at *p*H 7.2. The errors in these measurements are too small to show.

to explain the dependence of the RAS of this system on the potential applied to the Au(110) electrode.

It was suggested earlier that the dependence of the RAS profiles of adsorbed P499C on the potential applied to the Au(110) electrode arises from changes in the orientation of the isoalloxazine rings on the surface as the adsorbed molecules adopt different redox states [3]. Variations in the order in which the potentials were applied gave rise to irreversible changes in the RAS profiles that could be associated with conformational changes of the protein on the Au(110) surface [3].

In Fig. 3 the differences given by subtracting the RAS profile obtained at 0.056 V from those obtained following the sequence of applied potentials, −0.376, −0.465, −0.557, and −0.652 V, increase in this sequence across the whole spectral range. This is captured in Fig. 6 which shows the differences vary linearly with the applied potential with only slight variations in the slope at different energies.

Applying the model to the potential dependence of the P499C-Au(110) system we have from Eq. (2) for the RAS of this system at a particular applied potential V,

$$\Delta r^{(V)} = \Delta r(\mathrm{Au}^{(V)}) + \Delta r(L^{(V)}) + \Delta r(\mathrm{IR}^{(V)}). \quad (5)$$

Applying this to the results shown in Fig. 3 we have

$$\begin{aligned}\Delta r^{(V)}_{(\mathrm{P499C})} - \Delta r^{(0.056)}_{(\mathrm{P499C})} &= [\Delta r(\mathrm{Au}^{(V)}) - \Delta r(\mathrm{Au}^{(0.056)})] \\ &+ [\Delta r(L^{(V)}) - \Delta r(L^{(0.056)})] \\ &+ [\Delta r(\mathrm{IR}^{(V)}) - \Delta r(\mathrm{IR}^{(0.056)})]. \quad (6)\end{aligned}$$

The adsorption of P499C significantly reduces the dependence of the RAS of the Au(110) surface on the applied potential and to a certain extent "freezes" the Au(110) signal [3]. We assume this term cancels. The results of Fig. 3 show that the low-energy contribution, L, shows the same dependence on the applied potential as that of the isoalloxazine rings so we subsume this into the analysis of the contribution from the higher-energy features I and II arising from the isoalloxazine rings. We are left with

$$\begin{aligned}&\Delta r^{(V)}_{(\mathrm{P499C})} - \Delta r^{(0.056)}_{(\mathrm{P499C})} \\ &\quad = \Delta r(L^{(V)} + \mathrm{IR}^{(V)}) - \Delta r(L^{(0.056)} + \mathrm{IR}^{(0.056)}). \quad (7)\end{aligned}$$

The protein is known to open as it is successively reduced [10]. On the surface this is achieved by applying the successive, negative, redox potentials to the Au(110) electrode which is expected to steadily increase the angle α_1. This can be presented by increasing values of α_2. So for the first redox potential we have

$$\Delta r^{(-0.376)}_{(\mathrm{P499C})} - \Delta r^{(0.056)}_{(\mathrm{P499C})} = D_{L+\mathrm{IR}}(\cos\alpha_1 - \cos\alpha_2). \quad (8)$$

With $\alpha_2 > \alpha_1$ then the right-hand side of Eq. (8) will be positive for the whole range of angles indicated theoretically for the I and II transitions of the isoalloxazine rings and thus for the whole spectral range above 2.3 eV, as observed (Fig. 3). The same results hold for the low-energy contribution L suggesting that the orientation of the dipole moments of these transitions shows a similar dependence on the applied potential as those in the isoalloxazine rings. The application of successive redox potentials will steadily increase α_2 leading to increases in the spectral intensity across the whole spectral range as observed (Fig. 3). Furthermore since the cosine function shows a roughly linear decrease between 60° and 120° the linearity of the differences found at all energies shown in Fig. 6 suggests that successive redox potentials give rise to a roughly linear increase in α_2. The slight differences in the slopes shown in Fig. 6 at different energies show that the spectral features do not depend uniformly on the applied potential. The slope is notably different for the low-energy contribution, L (2.0 eV). The slight variation in slopes at different energies (Fig. 6) may indicate that the protein does not respond to changes in the applied potential as a rigid body and that the features that give rise to the contributions at different energies may not vary by exactly the same angle as the potential is varied.

As mentioned earlier the spectral differences shown in Fig. 4 show a different dependence on the applied potential compared to those shown in Fig. 3. In particular these differences do not vary linearly with the applied potential as can be seen in Fig. 7. The model makes it possible to explain the departure from the linear dependence of the spectral differences on the redox potential observed in Fig. 4 and shown in Fig. 7. In these experiments there will be a competition between successive decreases in the applied potential acting

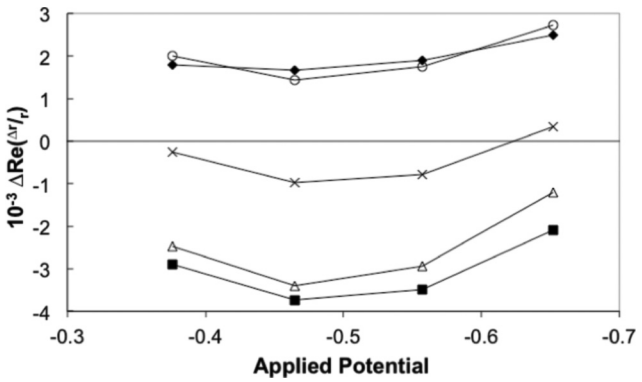

FIG. 7. Changes in peak intensity from Fig. 4 at 2.0 eV (♦), 2.6 eV (○), 3.0 eV (X), 3.6 eV (■), and 4.0 eV (△) as the P499C CPR + $NADP^+$ is reduced on the surface of the Au(110) electrode in 0.1*M* NaH_2PO_4-K_2HPO_4 at *p*H 7.2. The errors in these measurements are too small to show.

to reduce the P499C and the $NADP^+$ in solution acting to oxidize the protein. The former will act to open the molecule, increasing α_2, and the latter to close it; both processes will change the orientation of the FMN domain and hence the contribution of its isoalloxazine ring to the RAS profile. From the results (Fig. 7) it is clear that the balance of these two processes does not depend linearly on the applied potential. It may be that the behavior of the P499C adsorbed on the surface is determined by whichever of the nine redox forms of the protein can be populated by electrons from the electrode and whichever isoalloxazine ring can be reached by $NADP^+$ molecules at each value of the applied potential. The relative time scales of the oxidation and reduction processes may also be important. In this context it should be noted that each RAS experiment takes about 7 min. More insight into the time scale and the nature of the processes involved may be obtained from planned experiments with a rapid RAS instrument which can obtain spectra on a millisecond time scale [2,25].

V. CONCLUSION

The preceding analysis shows that the changes observed in the RAS profiles of monolayers of P499C adsorbed at Au(110)–electrolyte interfaces at 0.056 V following the addition of $NADP^+$ occur in regions of the spectrum that have been associated with changes induced in the orientation of the molecules on the Au(110) surface resulting from changes in the applied potential. For the spectral contributions associated with the isoalloxazine rings the changes observed in the RAS resulting from the addition of $NADP^+$ are expected to arise from changes in the orientations of the isoalloxazine rings with respect to the Au(110) surface, which implies that conformational changes similar to those identified in solution are occurring in the adsorbed molecules. A simple model based on the assumption that the FAD domain is fixed and that changes in the RAS profiles arise from rotations of the FMN domain and its accompanying isoalloxazine ring in a plane perpendicular to the surface and orientated along one of the principal directions of the Au(110) surface is able to account for the changes induced in the RAS profile as $NADP^+$ interacts with the adsorbed protein. This model also accounts for the changes observed in the RAS as the potential applied to the Au(110) surface is varied. The difference in the dependence of the RAS profile of the adsorbed protein on the potential applied to the electrode in the absence and presence of $NADP^+$ is explicable in terms of the model as arising from changes in the orientation of the isoalloxazine ring located in the FMN domain as a competition between the applied potential acting to reduce the protein and the $NADP^+$ to oxidize it. Future experiments with a faster instrument may provide insight into the time scales of these processes [2,25].

ACKNOWLEDGMENTS

P.W. acknowledges a useful discussion on the interpretation of the experimental results with Professor J. F McGilp of Trinity College, University of Dublin. The authors acknowledge financial support from the UK Biotechnology and Biological Science Research Council (BBSRC: Grants No. BB/F004400/1 and No. BB/F004397/1). J.H.C. was supported by a Ph.D. award funded by the UK Engineering and Physical Science Research Council. N.S.S. acknowledges support from an EPSRC Established Career Fellowship (EPSRC: Grant No. EP/J020192/1) and a Royal Society Wolfson Merit Award.

[1] H. L. Messiha, C. I. Smith, N. S. Scrutton, and P. Weightman, Europhys. Lett. **83**, 18004 (2008).
[2] J. H. Convery, C. I. Smith, B. Khara, N. S. Scrutton, P. Harrison, T. Farrell, D. S. Martin, and P. Weightman, Phys. Rev. E **86**, 011903 (2012).
[3] P. Weightman, C. I. Smith, J. H. Convery, P. Harrison, B. Khara, and N. S. Scrutton, Phys. Rev. E **88**, 032715 (2013).
[4] C. I. Smith, J. H. Convery, B. Khara, N. S. Scrutton, and P. Weightman, Phys. Status Solidi B **251**, 549 (2014).
[5] P. Weightman, G. J. Dolan, C. I. Smith, M. C. Cuquerella, N. J. Almond, T. Farrell, D. G. Fernig, C. Edwards, and D. S. Martin, Phys. Rev. Lett. **96**, 086102 (2006).
[6] C. I. Smith, A. Bowfield, G. J. Dolan, M. C. Cuquerella, C. P. Mansley, D. G. Fernig, C. Edwards, and P. Weightman, J. Chem. Phys. **130**, 044702 (2009).
[7] A. Bowfield, C. I. Smith, G. J. Dolan, M. C. Cuquerella, C. P. Mansley, and P. Weightman, e-J. Surf. Sci. Nanotechnol. **7**, 225 (2009).
[8] M. Wang, D. L. Roberts, R. Paschke, T. M. Shea, B. S. Masters, and J. J. Kim, Proc. Natl. Acad. Sci. USA **94**, 8411 (1997).
[9] S. Hay, S. Brenner, B. Khara, A. M. Quinn, S. E. J. Rigby, and N. S. Scrutton, J. Am. Chem. Soc. **132**, 9738 (2010).
[10] C. R. Pudney, B. Khara, L. O. Johannissen, and N. S. Scrutton, PLoS Biol. **9**, e1001222 (2011).
[11] S. Brenner, S. Hay, A. W. Munro, and N. S. Scrutton, FEBS J. **275**, 4540 (2008).
[12] P. Weightman, D. S. Martin, R. J. Cole, and T. Farrell, Rep. Prog. Phys. **68**, 1251 (2005).
[13] D. E. Aspnes, J. P. Harrison, A. A. Studna, and L. T. Florez, J. Vac. Sci. Technol. A **6**, 1327 (1988).
[14] C. I. Smith, A. Bowfield, N. J. Almond, C. P. Mansley, J. H. Convery, and P. Weightman, J. Phys.: Condens. Matter **22**, 392001 (2010).
[15] M. Salim, U. Siddiqui, G. Kodali, and R. J. Stanley, J. Phys. Chem. B **112**, 119 (2008).
[16] T. Climent, R. González-Luque, M. Merchán, and L. Serrano-Andrés, J. Phys. Chem. A **110**, 13584 (2006).
[17] L. B.-Å. Johansson, Å. Davidsson, G. Lindblom, and K. R. Naqvi, Biochemistry **18**, 4249 (1979).
[18] M. Sun, T. A. Moore, and P. S. Song, J. Am. Chem. Soc. **94**, 1730 (1972).
[19] The simple model yields the first term in Eq. (4). A more sophisticated analysis which takes into account the changes to the denominator in Eq. (1) using the approach of [20] and [21] modifies this to $2CD\ (\cos\alpha_2 - \cos\alpha_1) + D^2\ (\cos^2\alpha_2 - \cos^2\alpha_1)$ where C is a contribution which is probably dominated by the FAD domain and comparable in size to D. For $\alpha_2 > \alpha_1$ and α_1 in the range 60°–90° the first term dominates and the expression is negative for all reasonable values of α_2.

[20] D. S. Martin and P. Weightman, Surf. Interface Anal. **31**, 915 (2001).
[21] T. Farrell, P. Harrison, C. I. Smith, D. S. Martin, and P. Weightman, Appl. Phys. Lett. **93**, 191102 (2008).
[22] B. F. Macdonald and R. J. Cole, Appl. Phys. Lett. **80**, 3527 (2002).
[23] B. F. Macdonald, J. S. Law, and R. J. Cole, J. Appl. Phys. **93**, 3320 (2003).
[24] P. D. Lane, G. E. Isted, D. S. Roseburgh, and R. J. Cole, Appl. Phys. Lett. **95**, 141907 (2009).
[25] P. Harrison, T. Farrell, A. Maunder, C. I. Smith, and P. Weightman, Meas. Sci. Technol. **12**, 2185 (2001).